Aquatic Toxicology 231 (2021) 105732

Contents lists available at ScienceDirect

Aquatic Toxicology

journal homepage: www.elsevier.com/locate/aqtox

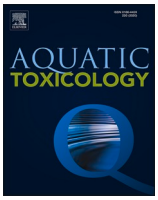

Characterization of river biofilm responses to the exposure with heavy metals using a novel micro fluorometer biosensor

Roberta Carafa [a,*], Nora Exposito Lorenzo [a], Jordi Sierra Llopart [b], Vikas Kumar [a,c], Marta Schuhmacher [a]

[a] Environmental Engineering Laboratory, Departament d'Enginyeria Quimica, Universitat Rovira i Virgili, Av. Països Catalans 26, 43007 Tarragona, Catalonia, Spain
[b] University of Barcelona Faculty of Pharmacy, Soil Science Unit, Campus Diagonal, Av. de Joan XXIII, 27-31, 08028 Barcelona, Spain
[c] IISPV, Hospital Universitari Sant Joan de Reus, Universitat Rovira I Virgili, Avinguda del Doctor Josep Laporte, 2, 43204 Reus, Spain

ARTICLE INFO

Keywords:
Toxicity
Heavy metal
Chemical speciation
River biofilm
EC50
Surface water monitoring

ABSTRACT

River biofilms are a suitable indicator of toxic stress in aquatic ecosystems commonly exposed to various anthropogenic pollutants from industrial, domestic, and agricultural sources. Among these pollutants, heavy metals are of particular concern as they are known to interfere with various physiological processes of river biofilm, directly or indirectly related to photosynthetic performance. Nevertheless, only limited toxicological data are available on the mechanisms and toxicodynamics of heavy metals in biofilms. Pulse Amplitude Modulated (PAM) fluorometry is a rapid, non-disruptive, well-established technique to monitor toxic responses on photosynthetic performance, fluorescence-kinetics, and changes in yield in other non-photochemical processes. In this study, a new micro-PAM-sensor was tested to assess potential acute and chronic effects of heavy metals in river biofilm. Toxicity values across the three parameters considered in this study (photosynthetic yield YII, non-photochemical quenching NPQ, and basal fluorescence F_0) were comparable, as determined EC50 were within one order of magnitude (EC50 ~1–10 mg L^{-1}). However, the stimulation of NPQ was more clearly associated with early acute effects, especially in illuminated samples, while depression of YII and F_0 were more prevalent in chronic tests. These results have implications for the development of functional indicators for the biomonitoring of aquatic health, in particular for the use of river biofilm as a bioindicator of water quality. In conclusion, the approach proposed seems promising to characterize and monitor the exposure and impact of heavy metals on river periphyton communities. Furthermore, this study provides a fast, highly sensitive, inexpensive, and accurate laboratory method to test effects of pollutants on complex periphyton communities that can also give insights regarding the probable toxicological mechanisms of heavy metals on photosynthetic performance in the river biofilm.

1. Introduction

It has been shown that micro-pollutants can have significant impacts on freshwater ecosystems and humans. Despite the significant efforts by regulatory bodies in the last decades to implement legislation for the protection of surface waters such as the European Water Framework Directive (WFD), pollution remains the main cause of water quality deterioration (Nõges et al., 2016). The establishment of ecological quality standards for a limited number of individual compounds does not enable the prediction of mixture toxicity, typical in environmental settings. One of the main issues in river monitoring is the inadequacy of monitoring data required to make informed decisions on regulating contaminant influxes into surface waters. This information lack is essentially due to the significant costs and time investments and to the insufficient time and spatial resolution of sampling efforts when using traditional grab sampling approaches. An incremented and improved water quality diagnosis capacity will also discourage abusive discharges. Data from the European Environmental Agency indicates that in 2018, 60 % of surface waters in Europe were in poor ecological status. In particular, many aquatic environments are highly affected by metal pollution, with copper (Cu), zinc (Zn), arsenic (As), lead (Pb), and nickel (Ni) being some of the most commonly detected contaminants in surface waters (Roig et al., 2015). The occurrence of metal contamination in fluvial ecosystems is commonly due to urban and mining activities

* Corresponding author.
E-mail address: roberta.carafa@fundacio.urv.cat (R. Carafa).

https://doi.org/10.1016/j.aquatox.2020.105732
Received 30 December 2019; Received in revised form 18 November 2020; Accepted 11 December 2020
Available online 24 December 2020

occurring in the respective watersheds (Corcoll et al., 2012). At the moment, Ecological Quality Standards (EQSs) in the WFD for heavy metals refer to the dissolved concentration (i.e., obtained after filtration of the water sample through a 0.45-μm filter). Uher et al. (2018) investigated the bioavailable concentrations of heavy metals in about one hundred sites throughout France and found bioavailable concentrations (based on data collected with DGT passive samplers) ranging from no detection to more than 1 mg L^{-1}. The concentrations of bioavailable heavy metals investigated in the present study can be compared to high exposure scenarios in Europe.

An estimate of the total cost of ecological monitoring of surface waters in the EU amounted to 350 million Euros/year (Lawson, 2005). The implementation of a more intense and complete water monitoring program remains a challenging task.

River biofilms are sensitive to exposure with micropollutants (Tiam et al., 2015) such as pesticides (e.g. Pesce et al., 2010), pharmaceuticals (e.g. Corcoll et al., 2014) and heavy metals (e.g. Serra et al., 2010;). Biofilms are considered to be good bioindicators and "early warning systems" for acute and chronic exposure to pollutants as demonstrated through analysis of functional descriptors such as photosynthesis efficiency or enzyme activity, and exposure leads to changes in community structure, respectively (Sabater et al., 2007). Stream biofilms are assemblies of bacteria, algae, diatoms, protozoa, and fungi surrounded by extracellular polymeric substances (EPS) that develop on and adhere to the riverbed and immersed materials. They are formed by phototrophic and heterotrophic communities, both of which are characterized by short generation times of hours to days. In lotic freshwater as well as marine ecosystems, periphytic biofilms support basic ecological functions such as primary production and nutrient cycling (Battin et al., 2003). Due to their structural complexity together with the fact that they are the first to interact with dissolved substances, river biofilms are particularly relevant for contamination assessment (Margoum et al., 2015). Several studies showed that several toxicants can inhibit algal photosynthesis (e.g. Schmitt-Jansen and Altenburger, 2008; Pesce et al., 2010; Corcoll et al., 2011) and indicated the sensitivity of river biofilms to heavy metals (e.g. Corcoll et al., 2012; Guasch et al., 2002; Xu et al., 2016; Tuulaikhuu et al., 2015; etc.). In particular, one of the main effects of metal toxicity is the inhibition of photosynthesis in autotrophic organisms (e.g. Serra et al., 2009; Corcoll et al., 2011).

Photosynthesis efficiency, also called photosystem II (PSII) Quantum Yield or photosynthetic yield, is the fraction of the calories adsorbed from radiation that is stored as calories of chemical potential. Two commonly used methods to measure photosynthesis inhibition are pulse-amplitude-modulation (PAM) fluorometry and the saturation pulse method. These approaches are based on the fact that light energy captured by photosynthetic pigments can be either: (i) used to drive photosynthesis, (ii) be dissipated as heat, or (iii) emitted as light (fluorescence). An increase in the yield of one process is directly linked to the decrease in the other two. It is therefore possible to measure a change in the efficiency of photochemical processes by measuring the yield of chlorophyll (or other pigments) fluorescence (Schreiber, 2004). The Pulse-Amplitude Modulation (PAM) fluorimeter operates with a specific modulation of the light signal that allows to detect only fluorescence excited by the measured light. This technique has proven to be very efficient for the detection of effects of metals as well as a range of other toxicants in microalgae (for a review e.g. Kumar et al., 2014). PAM fluorometry provides several advantages when assessing short- and long-term toxic effects on biofilm communities: (1) a combined and rapid evaluation of several functional parameters in parallel, (2) screening of trends over time, (3) observing effects in replication, and (4) being non-destructive (Schmitt-Jansen and Altenburger, 2008).

The principal limitation in the field application for this technique is the high variability of biofilm responses and the fact that variables not related to pollution can also influence photosynthetic parameters. This study aimed to test a new micro-PAM-sensor, that has been integrated into a monitoring device (Carafa et al., 2020, submitted patent num. 202030285), under laboratory conditions with the aim to contribute to its calibration for its intended use as an online in situ monitoring device. A detailed description of the monitoring device is presented elsewhere (Carafa et al., *in preparation*; Carafa et al., 2020, submitted patent num. 202030285), and here we provide a summary description to provide relevant context for this work. Specifically, the device consists of two chambers, one of which serves as a reference chamber with a purifying filter and a monitoring chamber with an inert filter to address the problem of biofilm variability. Both chambers house the biofilm and a fluorimeter, and measurements from both chambers are compared to identify changes in the aquatic environment. Having a local reference helps to avoid problems with differences in biofilm composition while testing at different sites/environments. In general, artificial biofilm communities are more resistant and have less biodiversity than natural biofilms, and for this reason, a natural biofilm collected from a pristine river was selected for toxicity tests in this study. Our objective for this study was to design and parameterize an inexpensive and effective protocol to identify acute and chronic toxicity due to exposure with heavy metals and ranges of sensitivity. Acute and chronic effects after 24−48 h and 1 week of exposure were analysed for exposures to 5 heavy metals: Cu, Zn, As, Pb and Ni. In addition, a short time (1 week) recovery test was performed in order to assess the recovery time of the biofilms after acute or short-term exposure, and which help us to calibrate the temporal resolution of the device to detect effects in the selected environment. The toxicity tests performed for heavy metals allowed addressing several issues related to: (i) differences in the toxicity of the selected heavy metals to river biofilms and characterization of their specific Mode of Action (MoA) and bioavailability; (ii) dose-response and time response of Chl-a fluorescence parameters as an early warning toxicity biomarker; (iii) relationships between the main regulatory mechanisms controlling the photosynthetic light reactions, the possible effects of heavy metals on these mechanisms and the effects measured in the selected PAM- parameters.

2. Materials and methods

2.1. Experimental setup and study site

The study was carried out in the Brugent, a calcareous stream tributary of a Mediterranean river, the Francolí, in Tarragona (NE Spain). The Brugent is a typical limestone stream with a basin area of 69 km^2, a mean slope of 2.9 %, a mean annual flow of 0.44 m^3s^{-1}, and a flood-peak discharge with a 500-year recurrence of 520 m^3s^{-1}. It is fed by water of karstic origin with alkaline pH, high concentrations of Ca and Mg, low electrical conductivity, and low nutrient and pollutant contents (Roig et al., 2013). Detail characterisation has been presented in Table S4 of the Supplementary material. Colonization of the biofilm was performed in the Brugent River on standard 75 by 25 mm microscope glass slides fixed to stainless-steel support during the months of January and February of 2019 (Fig. S1 in Supplementary material). Physico-chemical characteristics of the Brugent River were analysed before the study to ensure good water quality status. In particular, data from the Catalan Water Agency (ACA) surveillance and operational monitoring were used to select the site (Table S4 in Supplementary material). Values of major indexes of the biological quality of the river from ACA monitoring at the time of this study were: Specific Pollution Sensitivity Index (IPS) (Cemagref, 1982) = 13.4 for phytobenthos, Iberian Biomonitoring Working Party (IBMWP) (Hawkes, 1998) = 225 for macroinvertebrates and Index of Biotic integrity (IBICAT) (de Sostoa et al., 2010) = 9.57 for fish. The reference class values for the IPS, IBMWP, and IBICAT are presented in Table 1. In the laboratory, biofilm was maintained under the following conditions: Brugent river water collected from the colonization site and recirculated with an aquarium pump, natural solar photoperiod and illumination (maximum irradiance 418 μE m-2 s-1, average day length 14L:10D), pH 6.8 ± 0.1, room temperature (night--day fluctuation, min 15.9 °C, max 29 °C st. dev. 4 °C) and humidity

Table 1
Ranges of Specific Pollution Sensitivity Index (IPS), Specific Pollution Sensitivity Index (IBMWP) and Index of Biotic integrity (IBICAT) indices and respective water qualities and trophic status. Applicable categories for Brugent river data are highlighted in bold.

IPS	IBMWP	IBICAT	Water quality	Trophic status
>17	**>100**	>10,74	very good	oligotrophic
15–17	61-100	**>9,09**	good	oligo/mesotrophic
12–15	36-60	>6,30	satisfactory	mesotrophic
8–12	16-35	>2,57	poor	eutrophic
<8	<15	≤2,57	bad	hypertrophic

between 22 and 47 %. Two days before the begining of the test, each slide was carefully transferred into a Petri dish with nutrient-enriched modified Bold's Basal Medium (BBM) (non-autoclaved) medium. A liquid modified version of BBM pH 6.8 (Hydrochloric Acid -HCL was used to decrease the pH value to slightly acidic) was used for biofilm maintenance: the predominantly inorganic nature of this medium facilitates itself as an axenic-culture maintenance medium (Nichols and Bold, 1965).

2.2. Photosynthesis efficiency inhibition and recovery assays

Effects on photosynthesis efficiency were tested using a micro-PAM instrument (Heinz Walz GmbH, Germany) equipped with LEDs with a wavelength of 470 nm (technical description in Supplementary material S2). The test lasted 2 weeks and was performed in Petri dishes with BBM medium (control) or BBM medium spiked with test substances to a final volume of 25 ml. Media were replaced every two days. All reagents were purchased from Sigma AldrichTM (Saint Louis, MI, USA). Dilutions of single metals were prepared in distilled water (Table 2).

Biofilms were exposed to seven known concentrations of heavy metals (Cu, Zn, As, and Ni) ranging from 0.01 mM to 10 mM (spiked volume: 0.25 ml) with exception of Pb where 5 dilutions were prepared due to the lower solubility of this heavy metal (Table 2). Five blank controls were also added to the test battery. In order to measure always the same spot in each slide a numbered grid was added to the bottom of each Petri dish, as shown in Figure S3 (Supplementary material). On each biofilm slide four spots were measured (four replicates per treatment group). Effects were measured after acute and chronic exposures (24 h, 48 h, and one-week), and after one-week of recovery. Two sensors were used in parallel to measure two different points on each slide; the sensor measuring heads were placed immersed in the medium perpendicularly at 3.5 mm from the biofilm as shown in Figure S3 (Supplementary material). The Petri dishes were placed on a stirrer and a stirring bar was added during the test to ensure homogeneous mixing. A box was used to cover the samples for measurements in the dark phase.

After 6 min of dark-adaption, minimum fluorescence yield F_0 was measured on non-actinic measuring light (ML) with low intensity (3 µmol quanta $m^{-2}s^{-1}$ PAR, frequency 5 Hz, modulated pulses of 100 µsec). The Gain was adjusted such that in the absence of actinic illumination the fluorescence signal was in the range of a minimum 150–200 units. The saturation pulse has an intensity of 7700 µmol quanta m^{-2} s^{-1} PAR and lasts for 600 msec. Maximum fluorescence yield F_m, was measured after dark adaptation. Maximal PS II quantum yield (Max YII) was determined after dark adaptation and it was calculated as Max YII = F_v/F_m where F_v (= F_m-F_0) is the unquenched variable fluorescence. Four saturation pulses were applied each 60 s. maintaining the sample in the dark phase to check the homogeneity of the replicates. For acute tests, the test substances were added during a short break after pulse 2, maintaining the dark phase. The dark phase was maintained during 3 saturation pulses after the addition of the test substances and early effects on PS II were checked in the dark. Next, actinic light was applied at two PAR intensities: 25 and (after 5 min) 65 µmol quanta m^{-2} s^{-1} and further saturating pulses were given at intervals of 100 s. to measure the maximal level of fluorescence under illuminated conditions F_m'. The transient fluorescence, F_t, was monitored during the entire duration of the test: 5 min' dark adaptation plus 15 min test (5 min in dark, 5 min 25 PAR and 5 min 65 PAR). The effective PS II quantum yield was calculated by the formula: YII = (F_m'-F_0')/F_m', where F_0' is the level of fluorescence immediately before the saturation pulse (3 s. average). Only spots with a uniform covering of biofilm and basal fluorescence greater than 150–200 units were selected at the beginning of the tests in order to enhance homogeneity. The gain was set to 1 and damping to 2; the other PAM settings were left as default value of the instrument. The Stern-Volmer type non-photochemical fluorescence quenching (NPQ) (Bilger and Björkman, 1990), was calculated as NPQ = (F_M - $F_{M'}$)/$F_{M'}$.

2.3. Biofilm characterization

Biofilms were carefully removed from slides using a razor blade, then suspended in the BBM medium. The proportion of Diatoms and Chlorophyceae was determined by counting on a Neubauer chamber under a light microscope. The microscopy observations were performed with a magnitude of 100 X, 200 X, 400 X, 500 X for optical confocal microscope identification (Fig. 7 and Fig. S9, S10 in Supplementary material) and 5 X to 62 X for stereomicroscopic analysis (M205 C Stereo Microscope Leica) (Fig. 6). Sample preparation and taxonomic identification were performed following European standard NF EN 13946. Diatoms and Chlorophyceae were identified to the lowest taxonomic level possible using standard references (John et al., 2002; Guasch et al., 2002; Bellinger and Sigee, 2010, https://www.algaebase.org) and recent nomenclature updates.

2.4. Data processing

All data were log-transformed prior to data analysis to ensure the normality of data and homogeneity of variances. The results were fitted using the hormetic concentration-response model by Yoshimasu et al. (2015) implemented in Matlab R2017a. Hormesis in Concentration-response curves appears when an organism exhibits a biphasic response to toxicants exposure. Within the hormetic area, there is a favourable biological response to low exposures to toxicants with a maximum stimulation concentration (hEC), represented by the highest values of the concentration-response curve. Concentration-response graphs were also plotted in Matlab R2017a.

Metal speciation was simulated by Visual MINTEQ 3.1 (https://

Table 2
Tested single heavy metal dilutions (nominal concentrations in µg L^{-1} and corresponding concentration expressed in mM).

Heavy metal	As	Cu	Ni	Zn	Pb	Heavy metal	As, Cu, Ni, Zn	Pb
Source	$HAsNa_2O_4$	$CuSO_4$	$NiCl_2$	$ZnCl_2$	$PbCl_2$			
	7.49E+05	6.35E+05	5.87E+05	6.54E+05	4.14E+04		10	0.2
	3.75E+05	3.18E+05	2.94E+05	3.27E+05	2.07E+04		5	0.1
	1.50E+05	1.27E+05	1.17E+05	1.31E+05	1.04E+04		2	0.05
Tested dilutions (µg L^{-1})	7.49E+04	6.35E+04	5.87E+04	6.54E+04	2.07E+03	**Tested dilutions (mM)**	1	0.01
	3.75E+04	3.18E+04	2.94E+04	3.27E+04	1.04E+03		0.5	0.005
	1.50E+04	1.27E+04	1.17E+04	1.31E+04			0.2	
	7.49E+02	6.35E+02	5.87E+02	6.54E+02			0.01	

vminteq.lwr.kth.se/). This model is a chemical equilibrium model for the calculation of metal speciation, solubility equilibria, and sorption for natural waters.

3. Results

Values of the parameters of all fitted equations as well as the coefficients indicating the goodness of fit are listed in the Supplementary materials (Tables S6, S7 and S8).

3.1. Metal speciation

As the medium contains EDTA and other components that can chelate metal ions, only metal species that were bioavailable as well as effective concentrations and free ions were considered for deriving concentration-response curves.

Cu, Zn, and Ni showed the most complex behaviours: a) at a lower nominal concentration (~600 μg L^{-1}), they had a high sequestration rate by EDTA in common, and decreasing bioavailability, b) whereas at higher metal nominal concentrations (>600 μg L^{-1}), the EDTA was

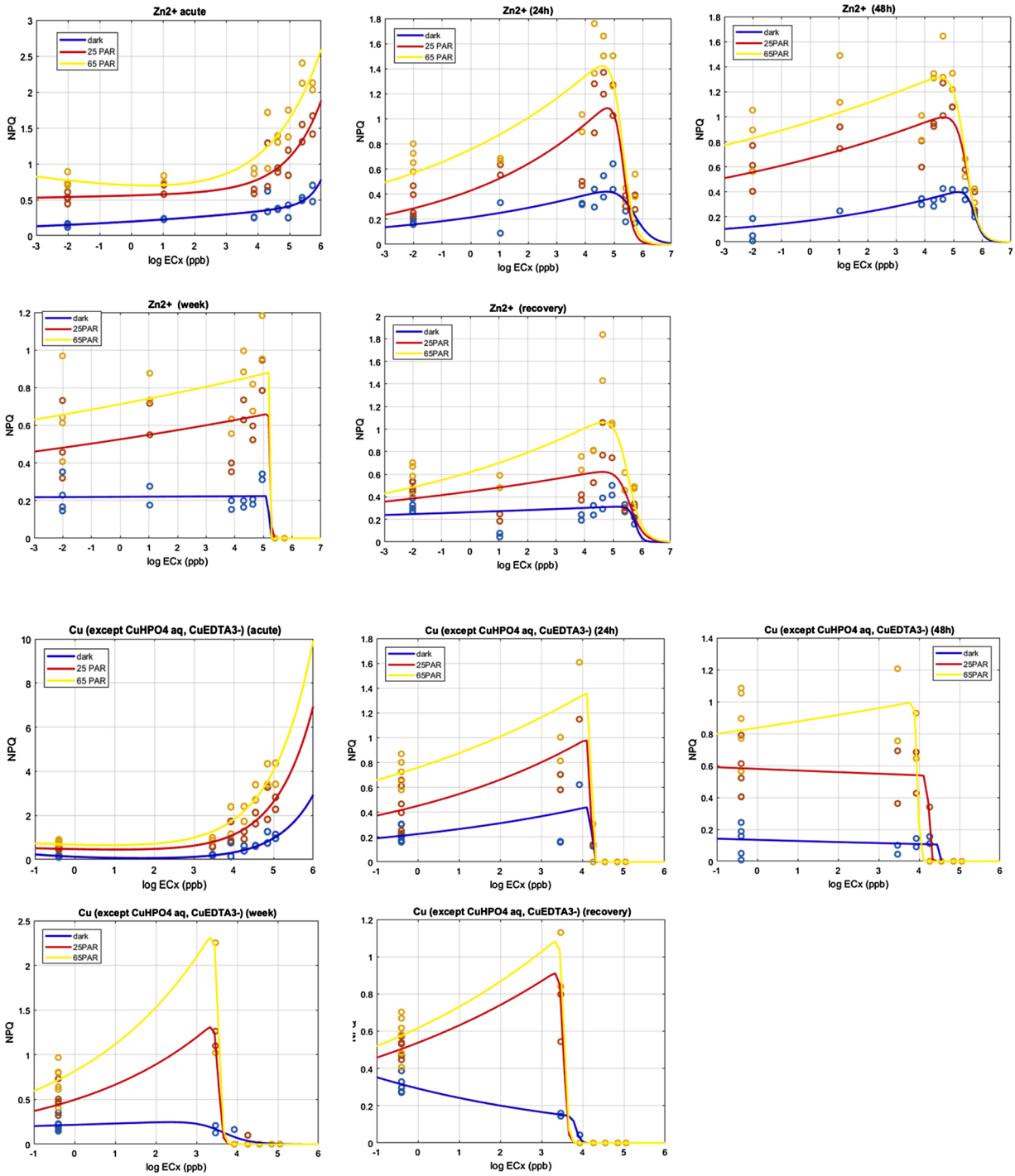

Fig. 1. NPQ concentration-response curves (lines) and experimental data (o) for Zinc and Copper exposed samples. Exponential model y = a*exp(b*x) + c*exp(d*x), DFE: 14. Hormetic model y = ((a–b)./(1+(exp((c* x)-d)))).(1+(exp((e*x)- f))). DFE: 12. Fit parameters in Matlab: MaxFunEvals = 6000; MaxIter = 40000; Robust = 'Bisquare'.

saturated and the most of Zn (>60 %) and Ni (>70 %) became bioavailable. In the case of Cu, metal bioavailability was ~60 % at very high nominal concentrations (~100 mgL^{-1}). As was dissolved and bioavailable as anions in all treatments. Pb forms a complex with EDTA (>99 %) up to 2,000 µg L^{-1}, and at higher concentrations (> 10,000 µg L^{-1}) Pb tends to become more bioavailable (>50 %). More details about metal speciation are available in supplemental materials (S5).

3.2. Non-photochemical quenching

In acute test cases, NPQ showed a clear stimulation in samples exposed to Zn, Cu, Ni and As (Figs. 1 and 2); in chronic tests, NPQ showed a hormetic behaviour with a narrow threshold between max stimulation and EC100 in samples exposed to Zn, Cu, and Ni (Figs. 1 and 2).

The observed pattern of the concentration-response curve for NPQ in the acute exposure experiment to Zn, Ni, Cu, and As was exponential (Figs. 1 and 2), while for Pb the data did not show any particular correlation (Fig. 3), due to its low bioavailable fraction (Fig. S5 in Supplementary material). Zn, Ni, and Cu showed a stimulation of NPQ at quite high concentrations (~log 10 mg L^{-1}, whereas for As first effects could be detected at ~log 1 mg L^{-1} ppb (Figs. 1 and 2). Light intensity affected the magnitude of the response. When more processes were activated in the cells, the effects of metals appeared more quickly

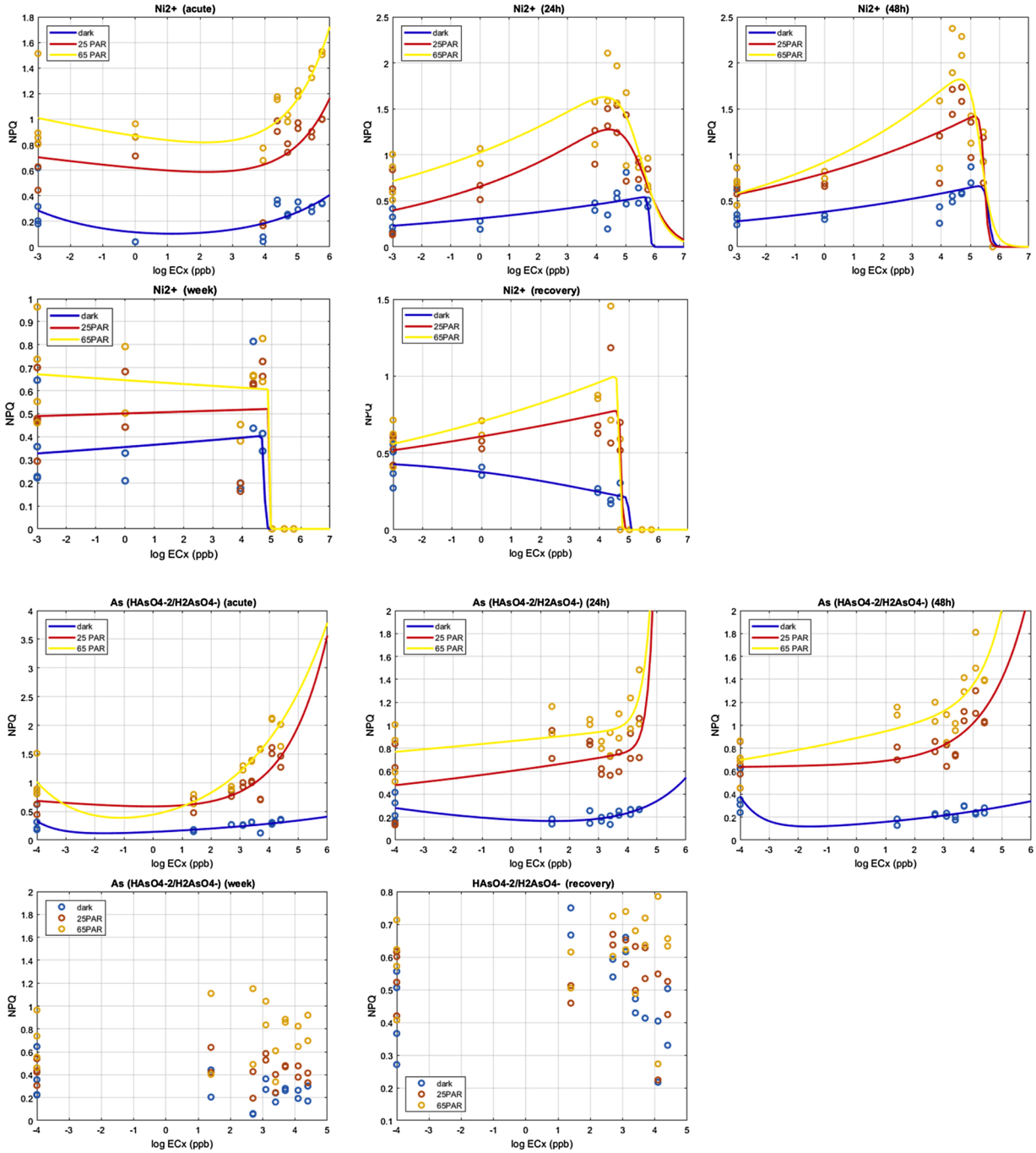

Fig. 2. NPQ concentration-response curves (lines) and experimental data (o) for Nickel and Arsenic exposed samples. Exponential model y = a*exp(b*x) + c*exp (d*x), DFE: 14. Hormetic model y = ((a–b)./(1+(exp((c* x)-d)))))./(1+(exp((e*x)- f))). DFE: 12. Fit parameters in Matlab: MaxFunEvals = 6000; MaxIter = 40000; Robust = 'Bisquare'.

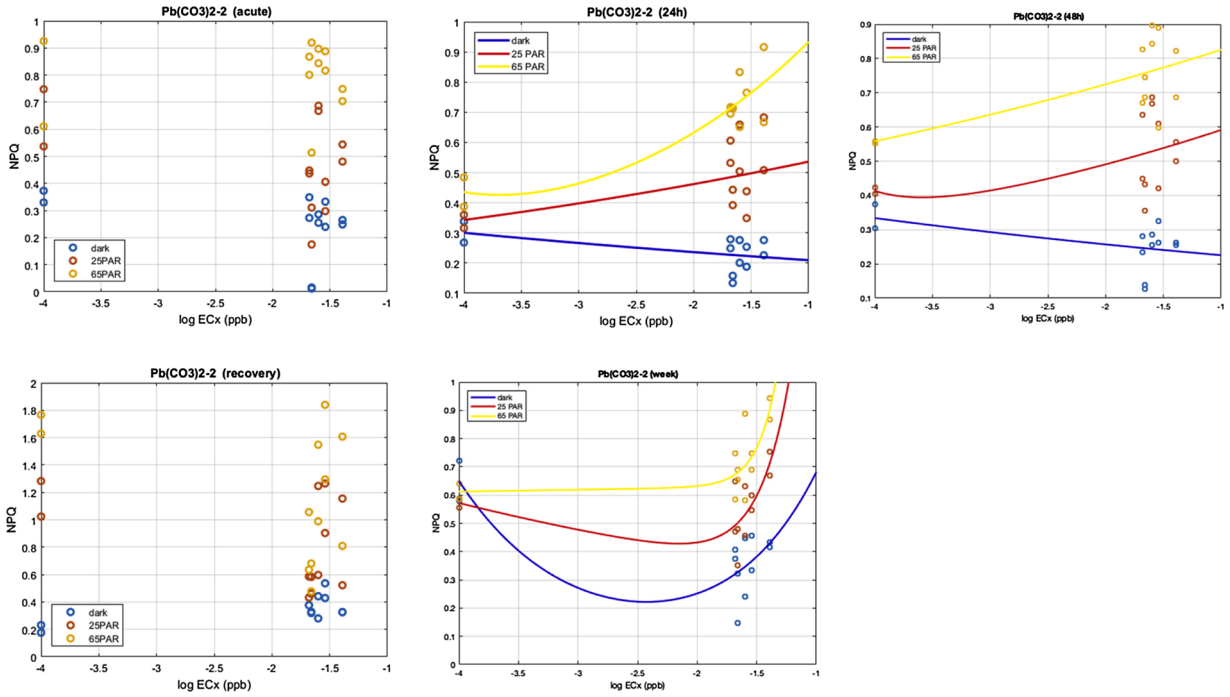

Fig. 3. NPQ concentration-response curves (lines) and experimental data (o) for Lead exposed samples. Exponential model y = a*exp(b*x) + c*exp(d*x), (DFE: 8). MaxFunEvals = 6000; MaxIter = 40000; Robust = 'Bisquare'.

(Figs. 1 and 2).

The concentration-response curves were very steep for Cu, Zn and Ni in most of the cases: at lower concentrations, the bioavailable fraction was reduced (Fig. S5). Chronic tests, in most of the cases, showed a clear hormetic effect (Figs. 1–3).

Zn had a more pronounced hormesis effect after short exposure time (24−48 h); however, after a week of exposure, the fitted curves showed a lower stimulation effect, where treatment concentrations were still very close to the EC50 showing higher values of NPQ (Fig. 1). After a week in the BBM medium, the biofilms that were exposed to higher Zn concentrations (> 10 mg L^{-1}) were able to partially recover (Fig. 1).

Chronic effects of Cu were more pronounced, especially for samples exposed to light, with lower values of EC50 (between ~1 and ~10 mg L^{-1}; Table 3). In the case of longer exposure duration (one week), the curve became very steep with values of maximum stimulation and EC50 values being very close and no recovery after a week of purification was observed.

Ni-exposed samples showed a behaviour very similar to those exposed to Cu, but the EC50 values were higher (> 10 mg L^{-1}; Table 3). Also, periphyton exposed to Ni at higher doses was not able to recover.

As and Pb exposed samples were not negatively affected by any treatment. As seemed to stimulate NPQ after acute, 24 and 48 h exposures (Fig. 2). A tentative exponential curve was also shown for Pb at 24−48 h and after the recovery period, but the correlation in this last case was very weak (Fig. 3).

3.3. Photosynthetic yield

YII was a sensitive parameter, especially in chronic tests after exposure to Zn, Cu, Ni and As (>1 mg L^{-1}) (Fig. 4). As expected for YII, light intensity positively affected the magnitude of the response (Fig. 4). Again, the hormetic model was used to fit the data but the hormetic effects were much less evident for YII in comparison to NPQ (Fig. 4).

Zn affected YII after acute exposure when samples were exposed to actinic light, in agreement with his MoA (PSII inhibitor). Regardless, the effects observed after acute exposures were very weak and the EC50 was much higher than environmental levels (> 1E07 mg L^{-1}) for samples exposed to 65PAR (Fig. 4; Table 4). Effects of Zn could also be seen after 24 h, and the effects measured after 48 h showed similar behaviour and comparable EC50 values, whereas after a week the curves appeared steeper (Fig. 4; Table 4). Also, for YII, samples exposed to Zn were able to recover after one week of depuration (Fig. 4).

Cu exposed samples showed some hormetic effect after the acute exposure. Similar to Zn, Cu affected YII in acute conditions only when samples were exposed to actinic light, but the effects were evident at lower concentrations in comparison to the effects of the other metals (Fig. 4; Table 4). The steepness of concentration-response curves after chronic exposure of Cu exposed samples were similar for 24−48 h and one week exposed samples and also after recovery, but lower values of EC50 were registered in comparison to Zn (Fig. 4; Table 4). In this case, cells were not able to recover, and the damage was irreversible.

Ni also showed a clear chronic effect on YII with EC50 values at about log 3 ppb at 65 PAR, but no significant acute effect was observed (Fig. 4; Table 4). The lowest EC50 value was registered after one-week exposure. In this case the activation of the photosynthesis seemed to slightly mitigate the effects of this metal. At 65 PAR the fit model predicted a hormetic effect after 24 and 48 h of exposure time with hEC equal to 0.01 μg $L^{-1}$and 0.02 μg L^{-1} (Fig. 4). Even if the r squared coefficient was high (0.917-0.942), and Root Mean Square Error (RMSE) was low (0.036-0.039), no data were available to confirm these affects at the predicted exposure concentrations. Also for Ni lowest EC50 values were observed after one week of exposure and recuperation was possible only for samples exposed to < 100 mg L^{-1}.

Small acute and chronic effects were observed for As exposed samples at a very high concentrations and only during illuminated tests, a complete recovery was observed after a week in clean medium (Fig. 4; Table 4).

Finally, for Pb exposed samples no clear response was observed; tentative fitting curves were drawn, showing a tendency of decrease of YII with higher Pb concentrations. However, bioavailability of this metal was low in all tested concentration, causing assembling of the point and lost in resolution; the Root Mean Square Error (RMSE) was very high (see Supplementary material, Table S5).

Table 3
The maximum stimulated concentration (hEC, mgL^{-1}) and the log half-maximal effective concentration (EC50, mgL^{-1}) of NPQ for Zn, Cu and Ni on pristine river biofilms. * indicate an exponential fit curve.

NPQ	Zn^{2+} dark		Zn^{2+} (25 PAR)		Zn^{2+} (65 PAR)	
	hEC	EC50	hEC	EC50	hEC	EC50
acute	n.d.*	n.d.*	n.d.*	n.d.*	n.d.*	n.d.*
24 h	59.84	1652.75	58.88	440.07	37.65	392.17
48 h	151.99	521.63	47.51	494.24	29.84	376.31
week	120.45	221.67	120.45	197.06	151.99	198.36
rec	151.99	720.08	37.65	610.06	47.51	693.84

NPQ	Cu (except $CuHPO_4$ aq, $CuEDTA^{3-}$) dark		Cu (except $CuHPO_4$ aq, $CuEDTA^{3-}$) 65PAR		Cu (except $CuHPO_4$ aq, $CuEDTA^{3-}$) 25PAR	
	hEC	EC50	hEC	EC50	hEC	EC50
acute	n.d.*	n.d.*	n.d.*	n.d.*	n.d.*	n.d.*
24 h	7.74	45.99	10.00	11.77	10.00	11.39
48 h	n.d.	9.39	n.d.	9.37	5.99	8.63
week	0.22	4.84	2.15	3.67	2.15	4.64
rec	n.d.	2.65	2.15	3.95	2.15	3.07

NPQ	Ni^{2+} dark		Ni^{2+} (25 PAR)		Ni^{2+} (65 PAR)	
	hEC	EC50	hEC	EC50	hEC	EC50
acute	n.d.*	n.d.*	n.d.*	n.d.*	n.d.*	n.d.*
24 h	385.35	703.80	29.84	3171.05	18.74	1281.49
48 h	191.79	498.97	151.99	353.59	47.51	499.60
week	37.65	57.29	75.65	90.95	n.d.	40.27
rec	1.00E-06	14.66	37.65	55.41	29.84	50.08

NPQ	$HAsO_4^{-2}/H_2AsO_4^-$ dark		$HAsO_4^{-2}/H_2AsO_4^-$ 25PAR		$HAsO_4^{-2}/H_2AsO_4^-$ 65PAR	
	hEC	EC50	hEC	EC50	hEC	EC50
acute	n.d.	n.d.	n.d.*	n.d.*	n.d.*	n.d.*
24 h	n.d.*	n.d.*	n.d.*	n.d.*	n.d.*	n.d.*
48 h	n.d.	n.d.	n.d.*	n.d.*	n.d.*	n.d.*
week	n.d.	n.d.	n.d.	n.d.	n.d.	n.d.
rec	n.d.	n.d.	n.d.	n.d.	n.d.	n.d.

NPQ	Pb^{2+} dark		Pb^{2+} 25PAR		Pb^{2+} 65PAR	
	hEC	EC50	hEC	EC50	hEC	EC50
acute	n.d.	n.d.	n.d.	n.d.	n.d.	n.d.
24 h	n.d.*	n.d.*	n.d.*	n.d.*	n.d.*	n.d.*
48 h	n.d.*	n.d.*	n.d.*	n.d.*	n.d.*	n.d.*
week	n.d.*	n.d.*	n.d.*	n.d.*	n.d.*	n.d.*
rec	n.d.	n.d.	n.d.	n.d.	n.d.	n.d.

3.4. Basal fluorescence

According to our results, the basal fluorescence F_0 of dark-adapted cells and F_0' for illuminated samples could also be used as an indicator of stress (Fig. 5and Table 5; Table S8 in Supplementary materials). Nevertheless, F_0 measured after dark adaptation and after acute exposure did not show any response in the acute tests for any metal, whereas for chronic exposures it seemed to be a good indicator of stress for Zn, Cu, and Ni (Fig. 5).

For Zn chronic exposures, F_0 at dark and F_0' for illuminated samples showed similar values, with increasing toxicity when samples were illuminated and with the lowest values of EC50 after a week exposure (from ~4 to ~10 mg L^{-1}) (Fig. 5 and Table 5). Also for this parameter a recovery after a week of purification was observed for Zn.

Cu chronic exposure showed lower values of EC50 (~1 mg L^{-1}) in comparison to other metals (Table 5) and no recovery was observed for samples exposed at levels higher than the EC50.

For Ni, acute effects were very low and no EC50 could be determined in the acute exposure experiment. However, for the chronic exposure experiment, EC50 values were between those measured for Zn and Cu (Table 5).

For As, only a decreasing tendency of the measured parameters was observed but the EC50 could not be calculated (Fig. 5).

Finally, for Pb again no clear effects were observed although the tentative hormetic model predicted some effects for F_0 at a concentration between 0.04 and 0.06 µg/L.

F_0 is directly correlated with Chl a content and thus to biomass in the sample (Eggert et al., 2006). Therefore, theoretically it can be used as an endpoint parameter after long-term exposure to detect changes in biofilm biomass. However, we also measured a decrease of F_0 after 24 h, which was a short time for detecting changes in biomass.

3.5. Biofilm species composition

The main species dominating the river biofilm colonising the glass slides were green algae: *Trentepohlia aurea* and *Trentepohlia* sp., *Printzina* sp., *Chlorochytrium* sp., *Klebsormidium flaccidum*, *Stigeoclonium tenue*, *Mougeotia* sp. (Fig. S9, S10 in Supplementary materials), *Trebouxia* sp., *Oedogonium* sp. (Fig. 7). Diatoms were present on top of green algae, in particular, the species: *Achnanthidium* sp. (Bacillariophyceae, Fig. 7), and to a lesser extent *Synedra* sp. and *Gomphonema* sp. The proportion of diatoms and chlorophyceae on the slides was about the same with a slight prevalence of chlorophyceae (3.28 × 10^ 7 org/cm2 chlorophyceae and 4.17 × 10^4 org/cm2 diatoms). Biofilms were analysed by optical confocal and stereoscopic microscopy again after the experiment, i.e. after the recovery period. Control biofilm showed diatoms growing on top of green algae forming multiple layers and a thick coverage. Biofilm exposed to Cu1mM showed some necrosis (Fig. 6), especially evident in the filamentous green algae. At very high concentrations the high amount of Cu incorporated by green algae could be visualised by its light blue colour (Fig. 6). Sample exposed to high Zn concentration lost the green spots that represent green algae (Fig. 6).

4. Discussion

The present study allowed to calibrate a micro-PAM sensor under laboratory conditions for its intended use as an online in situ monitoring device in the field. Through adjusting settings, we were able to verify the most interesting functional parameters to assess changes in biofilms exposed to heavy metals.

4.1. Metals speciation

In this study the tests were performed using BBM medium containing EDTA: the effect of EDTA on heavy metal toxicity is heavy metal- and EDTA concentration-dependent. Our results indicate that it is preferable to calculate the bioavailable percentage of heavy metals, as the binding effect of EDTA can significantly affect bioavailability. Nevertheless, speciation and metal binding alone do not explain the differences in metal toxicity. For example, As was not complexed with EDTA but showed lower toxicity. Other chemical and biological interaction also play an important role in the final toxicity. The complex speciation found for Cu, Zn and Ni can explain the steep concentration-response curves in our results. In fact, these metals were less bioavailable at a lower concentration (Table S5 in Supplementary material), leading to a sudden increase in bioavailability at higher concentrations.

4.2. Non-photochemical quenching

According to our results, NPQ is the parameter that reacts more quickly. It is stimulated during low and acute toxicity, and starts to be depressed when the cells are no longer able to detoxify. Some authors, in accordance with our results, found a decrease of the NPQ after long-term exposures of periphyton to Zn (Corcoll et al., 2011). The observed exponential pattern of the concentration response curve for NPQ in the acute exposure experiment to Zn, Ni, Cu and As could be explained considering that stress induced changes in light absorption caused by heavy metals can result in loss of excitation energy in the form of heat (Baker, 2008), indicated by the increase of the NPQ parameter. The

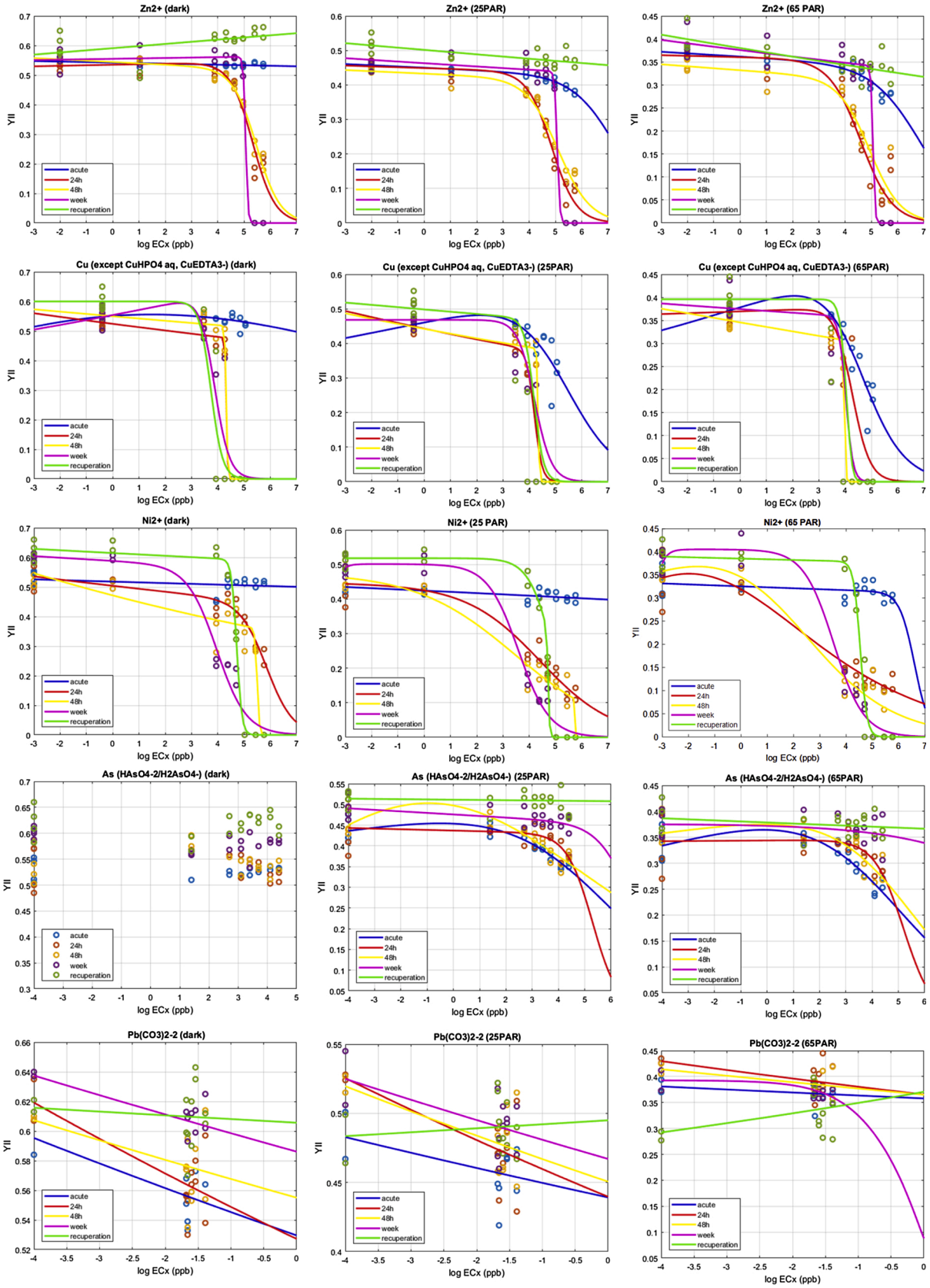

Fig. 4. YII concentration-response curves (lines) and experimental data (o) for Zn, Cu, Ni, As and Pb exposed samples. Hormetic model y = ((a–b)./(1+(exp((c* x)-d)))./(1+(exp((e*x)- f))). DFE: 12 (DFE 6 for Pb). Fit parameters in Matlab: MaxFunEvals = 6000; MaxIter = 40000; Robust = 'Bisquare'.

Table 4
The maximum stimulated concentration (hEC, mgL^{-1}) and the log half-maximal effective concentration (EC50, mgL^{-1}) of YII for Zn, Cu, Ni, As and Pb on pristine river biofilms.

YII	Zn^{2+} dark		Zn^{2+} (25 PAR)		Zn^{2+} (65 PAR)	
	hEC	EC50	hEC	EC50	hEC	EC50
acute	n.d.	n.d.	n.d.	1.85E+17	n.d.	11346.08
24 h	0.36	216.33	n.d.	66.09	n.d.	36.36
48 h	n.d.	259.96	n.d.	108.95	n.d.	59.42
week	47.51	106.99	n.d.	111.65	n.d.	19.27
rec	10000	n.d.	n.d.	n.d.	n.d.	n.d.

YII	Cu (except $CuHPO_4$ aq, $CuEDTA^{3-}$) dark		Cu (except $CuHPO_4$ aq, $CuEDTA^{3-}$) 25PAR		Cu (except $CuHPO_4$ aq, $CuEDTA^{3-}$) 65PAR	
	hEC	EC50	hEC	EC50	hEC	EC50
acute	0.03	1.91E+21	0.14	630.99	0.11	90.80
24 h	n.d.	38.31	n.d.	7.43	0.14	5.30
48 h	1.00E-06	2.77	n.d.	11.15	n.d.	6.12
week	0.36	5.58	n.d.	4.51	n.d.	3.04
rec	1.00E-06	4.56	n.d.	3.56	n.d.	3.04

YII	Ni^{2+} dark		Ni^{2+} (25 PAR)		Ni^{2+} (65 PAR)	
	hEC	EC50	hEC	EC50	hEC	EC50
acute	n.d.	n.d.	n.d.	n.d.	n.d.	n.d.
24 h	n.d.	495.74	n.d.	21.76	1.02E-05	2.44
48 h	n.d.	283.21	n.d.	6.45	2.06E-05	1.65
week	n.d.	0.41	1.71E-03	4.92	3.27E-05	4.65
rec	n.d.	32.28	n.d.	24.37	n.d.	22.27

YII	$HAsO_4^{-2}/H_2AsO_4^-$ dark		$HAsO_4^{-2}/H_2AsO_4^-$ 25PAR		$HAsO_4^{-2}/H_2AsO_4^-$ 65PAR	
	hEC	EC50	hEC	EC50	hEC	EC50
acute	n.d.	n.d.	2.78E-04	11573.20	7.74E-04	1328.13
24 h	n.d.	n.d.	n.d.	218.08	0.01	237.50
48 h	n.d.	n.d.	1.00E-04	45043.55	7.59E-04	1738.84
week	n.d.	n.d.	n.d.	1.41E+66	n.d.	n.d.
rec	n.d.	n.d.	n.d.	n.d.	n.d.	n.d.

YII	Pb^{2+} dark		Pb^{2+} 25PAR		Pb^{2+} 65PAR	
	hEC	EC50	hEC	EC50	hEC	EC50
acute	n.d.	n.d.	n.d.	n.d.	n.d.	n.d.
24 h	n.d.	n.d.	n.d.	n.d.	n.d.	n.d.
48 h	n.d.	n.d.	n.d.	n.d.	n.d.	n.d.
week	n.d.	n.d.	n.d.	n.d.	n.d.	4.75E-04
rec	n.d.	n.d.	n.d.	n.d.	n.d.	n.d.

medium term (one week) stimulation effect for treatment concentrations very close to the EC50 is also probably due to cells actively trying to detoxify (Fig. 1). Autotrophs have various responses to the toxic effects of heavy metals, such as selective metal uptake, metal binding, and induction of antioxidants (Kycko et al., 2019). The steepness of the NPQ concentration-response curves for Cu, Zn and Ni is probably linked to the speciation pattern. The mechanisms that are involved in the toxicity of heavy metals on photosynthesis are very complex and still a matter of speculation, but different authors agreed they involve electron transport in light reactions and enzyme activity in dark reactions (Kycko et al., 2019). This induced toxic stress together with the protective responses of cell metabolism can give an explanation of the behaviour of the NPQ in our tests. Due to its fast response after acute exposure (immediately after heavy metal addition), NPQ was identified as a promising early warning parameter.

4.3. Photosynthetic yield

YII is the most used parameter in PAM fluorometry and our results, indicating a decrease of this parameter in short term exposure experiments, are comparable with several studies in the literature. Corcoll et al. (2012) observed that, after few hours of exposure, metal toxicity measured as a decrease in YII, is more related to metal bioaccumulation than to metal concentration in water, which can explain the delay we found in the observed response. The lower photosynthetic performance of the community could depend on the direct toxicity of the metals but could also be attributed to the energetic cost of detoxification (Lavoie et al., 2016). The steep concentration-response curve for Zn exposed samples that we observed in our study could be explained, other than by metal speciation, also by bioaccumulation processes and the mode of action of Zn, targeting several photosynthetic processes of algae, diatoms and cyanobacteria (Admiraal et al., 1999). Long term effects on diatoms by Zn were also registered by Ivorra et al. (2002). Cu exposed samples showed some hormetic effect for YII after the acute exposure. This was expected as, even if Cu was toxic at high concentrations, Cu is essential as a component of algal enzymes (e.g. oxidases) and the electron transport chain (e.g. plastocyanin) (Pinto et al., 2003).

In the metabolism of photosynthetic organisms, Cu can show opposite effects: it is an essential micronutrient but at higher concentrations (>100 μg L^{-1}) or long exposure time it may become toxic (Serra et al., 2009). Chronic exposure to Cu is known to result in structural and functional effects in autotrophic and heterotrophic biofilm microbial communities (e.g. Boivin et al., 2006; Serra and Guasch, 2009; Serra et al., 2009).

The green microalgae *A. falcatus* is highly sensitive to Ni concentrations as low as 1 μg L^{-1}: photosynthetic pigments are reduced and Ni^{2+} increases antioxidant enzyme responses (Martínez-Ruiz and Martínez-Jerónimo, 2015). In our study EC50 values after chronic exposures to Ni (e.g. from ~1 to 5 mg L^{-1} for illuminated samples at PAR 65) were higher with respect to the values found in the literature for single species. However, they were in accordance with the study of Lawrence et al. (2004) in biofilms (0, 5 mg L^{-1} after the one-week exposure experiment).

Acute toxicity effects of As were previously observed on the photosynthetic efficiency of diatoms and cyanobacteria whereas green algae were less affected (Tuulaikhuu et al., 2015; Rodriguez Castro et al., 2014). Other As effects observed in river biofilms include growth reduction, less nitrogen content, higher dead diatom densities and a decrease in phototrophic component (Barral-Fraga et al., 2018). Exposure to an environmentally realistic concentration of As (120 μgL^{-1}) in an indoor experimental channels mimicking a fluvial system caused the following effects: decrease in the total biomass of biofilm and its potential ability to use organic P (i.e., phosphatase activity), inhibiting algal growth, especially that of diatoms, decreasing nitrogen content, and making the epipsammic biofilm more heterotrophic, thus reducing its ability to oxygenate the aquatic environment (Tuulaikhuu et al., 2015). The toxicity we measured for As was very low with respect to the other heavy metals (except Pb). Taking into account the listed previous studies, probably the justification of our results is linked to the specific species sensitivities in our biofilms.

For Pb, de Oliveira Gonçalves Alho et al. (2019) found an IC50–72 h of 0.78 μM and measured significant changes of chlorophyll-a synthesis and a reduction of both efficiencies of oxygen-evolving complex and quantum yields. In our study, Pb didn't affect biofilms, but for this metal the sequestration rate by EDTA was important: in this case, it would be probably better to perform the test in a modified medium with lower or no EDTA. However, in this case, the effects of lack of EDTA have to be also considered, to avoid biased results. Mineralization of Lead on EPS produced by cells in biofilms may occur in natural environments and was assessed in the laboratory by Couasnon et al. (2019).

4.4. Basal fluorescence

In general, basal fluorescence F_0 and F_0'are not considered in toxicity tests. In our study, F_0 seems to produce robust data after chronic exposures with the advantage to be easier to measure compared to NPQ and YII, as F_0 do not require an induction curve for its calculation.

A mechanistic explanation of the basal fluorescence results is not easy to formulate, as fluorescence is linked to many physiological

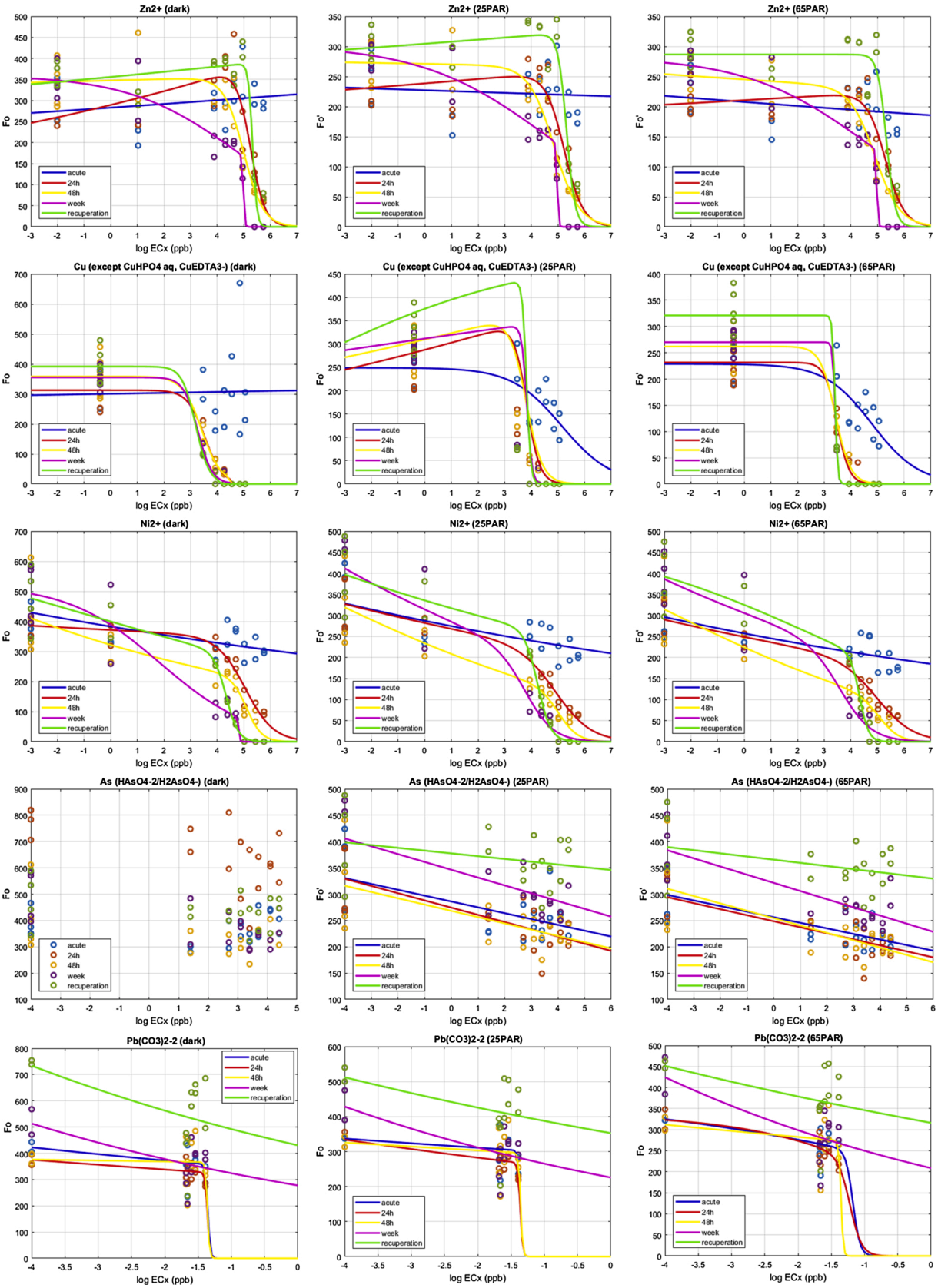

Fig. 5. F_0 concentration-response curves (lines) and experimental data (o) for Zn, Cu, Ni, As and Pb exposed samples. Hormetic model y = ((a–b)./(1+(exp((c* x)-d)))./(1+(exp((e*x)- f))). DFE: 12 (DFE: 6 for Pb). Fit parameters in Matlab: MaxFunEvals = 6000; MaxIter = 40000; Robust = 'Bisquare'.

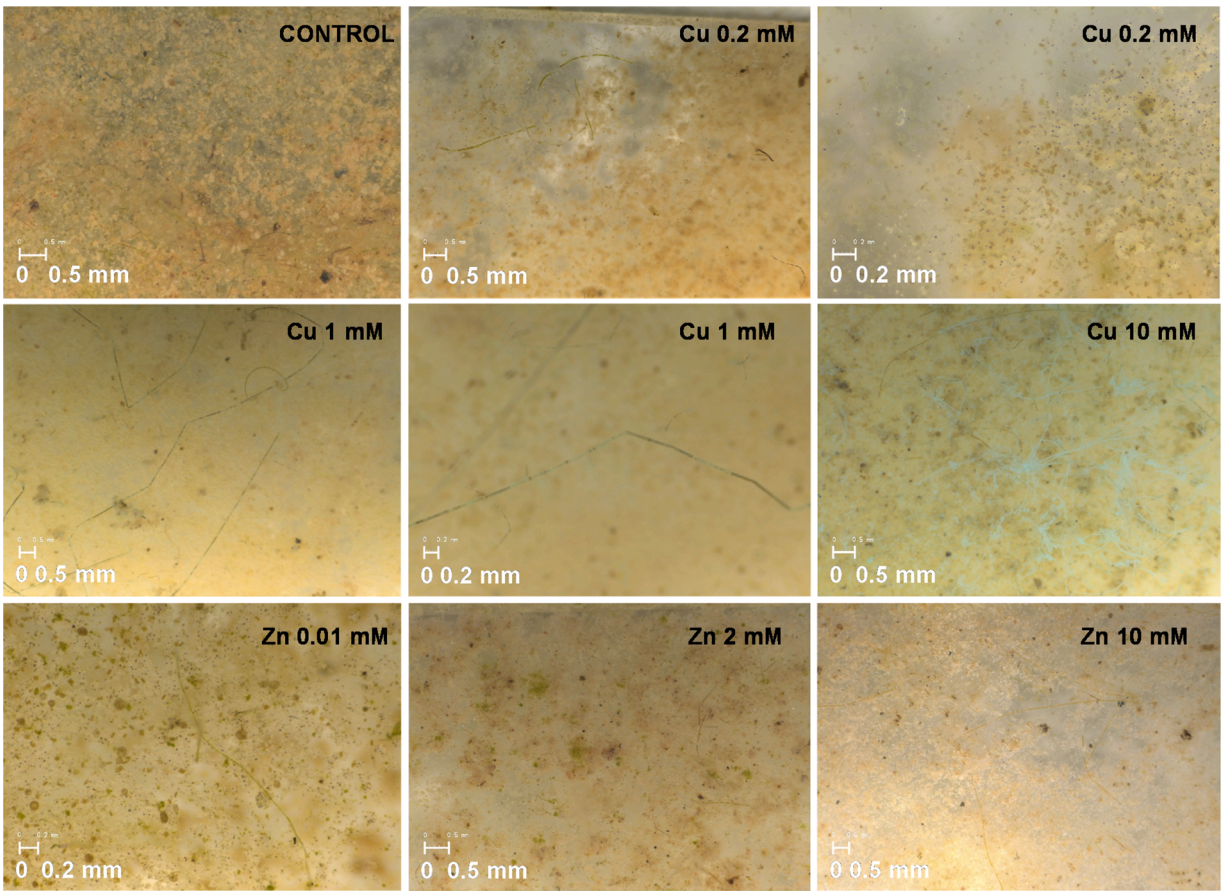

Fig. 6. Pictures of selected biofilms at stereoscopic microscope after the recovery period. Exposure concentrations are indicated on the upper right.

processes affected by heavy metals: stress-induced decreases in stomatal conductance, carbon metabolism, and transport processes can all affect PSII efficiency inducing changes in absorbed light energy use and consequently in fluorescence (Schreiber, 2004). In addition, metal exposure can result in increases in concentrations of reactive oxygen species (ROS) that can cause a change in signal transduction, which affects expression of genes, changes the properties of the membranes, and also damages photosystem II (PSII) (e.g. Aro et al., 2005). These toxic effects induced by heavy metals may directly or indirectly affect basal fluorescence.

Xu et al. (2016) found significant differences in the photosynthetic quantum yields following exposure to 3.89 and 7.85 mg L^{-1} Zn^{2+} for 6 h, and after 21 days noticeable changes in community composition occurred (i.e., substantial loss of diatoms). These values are in accordance with the EC50 values of F_0 measured in this study (~4 to ~10 mg L^{-1}) after one-week exposure to Zn.

The concentration ranges of toxicity of physiological essential heavy metals depend on many factors including organism species and the oxidation state of microelement. For example, Mykhaylenko and Zolotareva (2017) found that the addition of 0.67−4 mg L^{-1} of Cu nanocarboxylates resulted in an increase in *Chlorella* biomass by approximately 20 %; however, concentrations ranging between 20 and 40 mg L^{-1} strongly inhibited algal growth after the 12th day of cultivation. Guasch et al. (2002), found that Cu exposure of periphyton of oligotrophic calcareous rivers at 10–20 μg/L (12 days of exposure) caused stronger effects on structural (algal biomass and community structure) than on functional (photosynthetic efficiency) parameters of periphyton. Exposure to Cu for 96 h induced significant growth differences in the diatom *Tabellaria flocculosa* at 6 and 10 μg/L, with approximately 50 % and 70 % growth inhibition, respectively and increase in oxidative stress (Gonçalves et al., 2018). In our study we found higher EC50 values of ~1−2 mg L^{-1} after chronic exposure to Cu, indicating that probably a biofilm from oligotrophic calcareous rivers could be even more sensitive in detecting metal pollution than the biofilm investigated in this study.

Lawrence et al. (2004), in a one-week exposure experiment, found that some effects of Ni in biofilms were the elimination of cyanobacterial populations and reduced photosynthetic biomass in the biofilms. In the same study, Ni at 0.5 mg L^{-1} resulted in reductions in carbon utilization; the presence of Ni eliminated the positive influence of nutrients on the biofilms. This study is generally in agreement with our results indicating a reduction of F_0 after Ni chronic exposure; however, the measured EC50 in our study for were higher (~3.5 mg L^{-1} after one-week exposure).

Our study together with the mentioned literature studies could justify the use of basal fluorescence, which is correlated with algal biomass, as an endpoint after chronic heavy metals exposure and confirm in part our data. However, we measured a decrease of F_0 also after short time exposure (24 h). More laboratory and modelling studies taking into account algal physiology are needed to better understand the behaviour of this parameter.

4.5. Biofilm species composition

The species identified in the biofilms were typical of pristine river biofilms from a low impacted area. The biofilm was highly patchy, but as the measured parameters were derived from a ratio of fluorescence intensities, inhomogeneity of fluorescence excitation intensity or chlorophyll concentration was not of relevance and remaining inhomogeneity could be interpreted in terms of differences in photosynthetic performance. In the environment part of the recovery process is due to re-colonization with organisms coming from the upstream while in the laboratory conditions are no other sources of microorganisms,

Table 5
The maximum stimulated concentration (hEC, mgL^{-1}) and the log half-maximal effective concentration (EC50, mgL^{-1}) of F_0 for Zn, Cu, Ni, As and Pb on pristine river biofilms.

F_0	Zn^{2+} dark		Zn^{2+} (25 PAR)		Zn^{2+} (65 PAR)	
	hEC	EC50	hEC	EC50	hEC	EC50
acute	n.d.	n.d.	n.d.	n.d.	n.d.	n.d.
24 h	11.77	258.58	2.31	195.20	2.31	220.73
48 h	0.45	101.50	n.d.	68.54	n.d.	32.54
week	n.d.	4.001	n.d.	10.26	n.d.	9.98
rec	59.95	220.70	18.74	221.38	n.d.	217.37

F_0	Cu (except $CuHPO_4$ aq, $CuEDTA^{3-}$) dark		Cu (except $CuHPO_4$ aq, $CuEDTA^{3-}$) 25PAR		Cu (except $CuHPO_4$ aq, $CuEDTA^{3-}$) 65PAR	
	hEC	EC50	hEC	EC50	hEC	EC50
acute	n.d.	n.d.	n.d.	196.74	n.d.	54.33
24 h	n.d.	3.28	0.57	2.81	n.d.	2.82
48 h	n.d.	2.80	0.28	2.88	n.d.	2.78
week	n.d.	2.33	1.83	0.83	n.d.	0.96
rec	n.d.	2.02	2.31	0.69	n.d.	0.94

F_0	Ni^{2+} dark		Ni^{2+} (25 PAR)		Ni^{2+} (65 PAR)	
	hEC	EC50	hEC	EC50	hEC	EC50
acute	n.d.	n.d.	n.d.	n.d.	n.d.	n.d.
24 h	n.d.	68.96	n.d.	27.51	n.d.	28.48
48 h	n.d.	20.51	n.d.	8.57	n.d.	7.62
week	n.d.	19.46	n.d.	3.34	n.d.	3.47
rec	n.d.	0.96	n.d.	9.96	n.d.	9.03

F_0	$HAsO_4^{-2}/H_2AsO_4$-dark		$HAsO_4^{-2}/H_2AsO_4$-25PAR		$HAsO_4^{-2}/H_2AsO_4$-65PAR	
	hEC	EC50	hEC	EC50	hEC	EC50
acute	n.d.	n.d.	n.d.	n.d.	n.d.	n.d.
24 h	n.d.	n.d.	n.d.	n.d.	n.d.	n.d.
48 h	n.d.	n.d.	n.d.	n.d.	n.d.	n.d.
week	n.d.	n.d.	n.d.	n.d.	n.d.	n.d.
rec	n.d.	n.d.	n.d.	n.d.	n.d.	n.d.

F_0	Pb^{2+} dark		Pb^{2+} 25PAR		Pb^{2+} 65PAR	
	log hEC	log EC50	log hEC	log EC50	log hEC	log EC50
acute	n.d.	4.23E-05	n.d.	4.23E-05	n.d.	6.14E-05
24 h	n.d.	4.64E-05	n.d.	4.38E-05	n.d.	5.09E-05
48 h	n.d.	5.09E-05	n.d.	4.52E-05	n.d.	4.54E-05
week	n.d.	n.d.	1.00E-07	n.d.	n.d.	n.d.
rec	n.d.	n.d.	1.00E-07	n.d.	n.d.	n.d.

consequently the recovery solely depends on the ability of the periphyton to detoxify. Effects on changes in the community and possible adaptation can appear in the field, this community shift may affect the sensitivity of the biofilms and of the tested sensor in detecting acute contamination events. For example, in the case of Zn and As exposure, a recovery in biofilm functional parameters was observed after one week in a clean medium in this study. Lambert et al. (2012) found that changes in biofilm microbial communities generally lead to an increase in community tolerance to metals. Anyway, these changes take time to produce a complete recovery. Lambert et al. (2012) reported that it took six weeks for a complete recovery after exposure of a river biofilm to Cu, and only when immigration from pristine not affected communities was possible. Corcoll et al. (2012) measured recovery from Zn exposure after three to five weeks; this recovery was also explained by changes in the community composition.

More experiments under field conditions are needed to evaluate the magnitude of the possible adaptation of biofilm communities to heavy metal toxicity.

4.6. *Performance of the overall test system*

Overall, the micro-PAM sensor used in this study is tailored to field measurements due to its compact measuring head, its waterproof housing, its low energy demand and its low price (~5,000 Euros) compared to more complex PAM systems such as IMAGING-PAM (~25,000 Euros). The performed tests in laboratory were useful to verify the performance of this sensor under controlled conditions. Micro-PAM is suited in particular for small samples and its use on river biofilm is appropriate, as demonstrated by this study.

However, more research is needed in order to evaluate the sensitivity and the temporal variability of the micro-PAM sensor and the associated monitoring device under field conditions. Based on the laboratory results it seems preferable to use high PAR intensities, close to saturation, in order to obtain more rapid and clear results. Toxicity values derived for the three parameters considered in this study (YII, NPQ, and F_0) were comparable and within one order of magnitude. It should be noted that they give complimentary information if we look at the different curves fitting. Therefore, it is recommended to measure a combination of at least two endpoints, YII and NPQ, because these provide complementary parameters on chronic and acute effects.

5. Conclusions

Early effects of exposure to heavy metals include impairments of river biofilm functions, supporting the use of Chla fluorescence techniques as signals of early toxicity. In this study, two new parameters, basal fluorescence F_0 and non-photochemical quenching NPQ, are suggested as indicators of possible contamination events because of their ease of measurement. Additionally, YII, traditionally used to assess the effects of metals on the photosystem, was also included as an endpoint. The suitability of the new micro-PAM sensor to assess early effects of

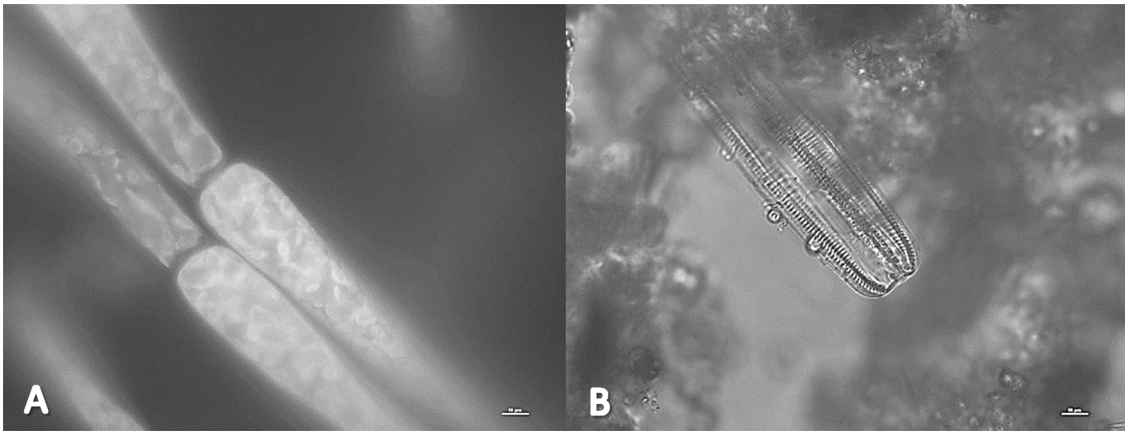

Fig. 7. Confocal images of filamentous Chlorophytes and Diatom from biofilm samples. A: 400 X, 633 nm, *Oedogonium* sp. B: 400X, white light, Bacillariophyceae.

zinc, copper, nickel, arsenic, and lead in river biofilms was shown in our case study where stimulation of NPQ was shown to represent a clear acute effect, especially in illuminated samples, and depression of YII and F_0 were demonstrated to represent useful endpoints especially in chronic tests. NPQ showed a clear hormetic behaviour in chronic tests with a narrow threshold between max stimulation and EC100. The next steps to validate this sensor and the associated monitoring device will be a comparative study to test its sensitivity compared with other PAM instruments. This sensor will further be tested to assess the sensitivity of biofilm communities to pharmaceuticals and pesticides, to calibrate it in the field in selected rivers and WWTP outflows and to assess mixture effects and site-specific differences in biofilm sensitivity and composition. Chla fluorescence in biofilm appears to be particularly useful for short term pollution detection, suggesting this parameter may be useful for detecting recent contamination and in online monitoring. A further improvement of the sensor will be the implementation of measurements at a different wavelength that will allow the detection of effects more specifically in diatoms and cyanobacteria. This study, as a first step in the calibration of a continuous monitoring device, is of interest for its possible application in EU monitoring programs. Nevertheless, more research is needed to test the microsensor in the field and validate the results obtained in laboratory assays.

Declaration of Competing Interest

The authors declare that they have no known competing financial interests or personal relationships that could have appeared to influence the work reported in this paper.

CRediT authorship contribution statement

Roberta Carafa: Conceptualization, Methodology, Formal analysis, Project administration, Funding acquisition, Writing - original draft, Writing - review & editing, Visualization, Data curation, Investigation, Validation. **Nora Exposito Lorenzo:** Methodology, Resources, Formal analysis. **Jordi Sierra Llopart:** Software, Supervision. **Vikas Kumar:** Software, Supervision. **Marta Schuhmacher:** Supervision, Resources.

Acknowledgements

The authors thank the Tecniospring Plus programme and ACCIÓ for funding this project. This project has received funding from the European Union's Horizon 2020 research and innovation programme under the Marie Skłodowska-Curie grant agreement No 712949 (grant number: TECSPR17-1-0012). Xavier Gomara Barbera from URV, supported part of the laboratory analysis. V. Kumar received funds from Health Department of Catalonia Government trough"Pla Estratègic de Recerca i Innovació en salut" (PERIS 2016-2020).

Appendix A. Supplementary data

Supplementary material related to this article can be found, in the online version, at doi:https://doi.org/10.1016/j.aquatox.2020.105732.

References

Admiraal, W., Blanck, H., Jong, M., Guasch, H., Ivorra, N., Lehmann, V., Nyström, B.A. H., Paulsson, M., Sabater, S., 1999. Short-term toxicity of zinc to microbenthic algae and bacteria in a metal polluted stream. Water Res. 33, 1989–1996.

Aro, E.M., Suorsa, M., Rokka, A., Allahverdiyeva, Y., Paakkarinen, V., Saleem, A., Battchikova, N., Rintamäki, E., 2005. Dynamics of photosystem II: a proteomic approach to thylakoid protein complexes. J. Exp. Bot. 56, 347–356.

Baker, N.R., 2008. Chlorophyll fluorescence: a probe of photosynthesis in vivo. Annu. Rev. Plant Biol. 59, 89–113. https://doi.org/10.1146/annurev.arplant.59.032607.092759.

Barral-Fraga, L., Martiñá-Prieto, D., Barral, M.T., Morinc, S., Guasch, H., 2018. Mutual interaction between arsenic and biofilm in a mining impacted river. Sci. Total Environ. 636, 985–998.

Battin, T.J., Kaplan, L.A., Newbold, J.D., Hansen, C.M.E., 2003. Contributions of microbial biofilms to ecosystem processes in stream mesocosms. Nature 426, 439–441.

Bellinger, E.G.G., Sigee, D.C., 2010. Freshwater Algae: Identification and Use As Bioindicators. John Wiley & Sons, Ltd, 118 pp.

Bilger, W., Björkman, O., 1990. Role of the xanthophyll cycle in photoprotection elucidated by measurements of light-induced absorbance changes, fluorescence and photosynthesis in leaves of *Hedera canariensis*. Photosyn. Res. 25, 173–185.

Boivin, M.E.Y., Massieux, B., Breure, A.M., Greve, G.D., Rutgers, M., Admiraal, W., 2006. Functional recovery of biofilm bacterial communities after copper exposure. Environ. Pollut. 140, 239–246.

Carafa, R., Gallé, T., Sierra Llopart, J., Vázquez Vilamajó, L., 2020. Dispositivo de monitorización de sustancias tóxicas en agua y sistema que lo comprende. Solicitud de Patente Nacional en España No 202030285. S/Ref.: N/Ref.: 2019/51535.

Cemagref, 1982. Etude des Methodes Biologiques d'Appreciation Quantitative de la Qualité des Eaux. Rapport Q.E. Lyon. Agence de 'Eau Rhone-Mediterranée-Corse –Cemagref, Lyon, France.

Corcoll, N., Bonet, B., Leira, M., Guasch, H., 2011. Chl-a fluorescence parameters as biomarkers of metal toxicity in fluvial biofilms: an experimental study. Hydrobiologia 673, 119–136.

Corcoll, N., Bonet, B., Morin, S., Tlili, A., Leira, M., Guasch, H., 2012. The effect of metals on photosynthesis processes and diatom metrics of biofilm from a metal-contaminated river: a translocation experiment. Ecol. Indic. 18, 620–631.

Corcoll, N., Casellas, M., Huerta, B., Guasch, H., Acuña, V., Rodríguez-Mozaz, S., Serra-Compte, A., Barceló, D., Sabater, S., 2014. Effects of flow intermittency and pharmaceutical exposure on the structure and metabolism of stream biofilms. Sci. Total Environ. 503-504 (15), 159–170. https://doi.org/10.1016/j.scitotenv.2014.06.093.

Couasnon, T., Gélabert, A., Ona-Nguema, G., Zanna, S., Ménez, B., Guyot, F., 2019. Experimental assessment of occurrences and stability of lead-bearing minerals in bacterial biofilms. Chem. Geol. 505, 23–35.

de Oliveira Gonçalves Alho, L., Castelhano Gebara, R., de Araujo Paina, K., Sarmento, H., da Graça Gama Melão, M., 2019. Responses of *Raphidocelis subcapitata*exposed to Cd and Pb: mechanisms of toxicity assessed by multiple endpoints. Ecotoxicol. Environ. Saf. 169, 950–959.

de Sostoa, A., Caiola, N., Casals, F., García-Berthou, E., Alcaraz, C., Benejam, L., Maceda, A., Solà, C., Munné, A., 2010. Ajust de l'Índex d'Integritat Biòtica (IBICAT) basat en l'ús dels peixos com a indicadors de la qualitat ambiental als rius de Catalunya. https://doi.org/10.13140/2.1.1551.6964.

Eggert, A., Häubner, N., Klausch, S., Karsten, U., Schumann, R., 2006. Quantification of algal biofilms colonising building materials: chlorophyll a measured by PAM-fluorometry as a biomass parameter. Biofouling 22 (2), 79–90. https://doi.org/10.1080/08927010600579090.

Gonçalves, S., Kahlert, M., Almeida, S.F., Figueira, E., 2018. Assessing Cu impacts on freshwater diatoms: biochemical and metabolomic responses of *Tabellaria flocculosa* (Roth) Kützing. Sci. Total Environ. 625 (1), 1234–1246.

Guasch, H., Paulsson, M., Sabater, S., 2002. Effect of copper on algal communities from oligotrophic calcareous streams. J. Phycol. 38, 241–248.

Hawkes, H.A., 1998. Origin and development of the biological monitoring working party score system. Water Res. 32 (3), 964–968.

Ivorra, N., Barranguet, C., Jonker, M., Kraak, M.H.S., Admiraal, W., 2002. Metal-induced tolerance in the freshwater microbenthic diatom *Gomphonema parvulum*. Environ. Pollut. 116, 147–157.

John, D.M., Whitton, B.A., (Editors), Brook A.J., 2002. The Freshwater Algal Flora of the British Isles An Identification Guide to Freshwater and Terrestrial Algae Field / Identification Guide Identification Key, 878 pp.

Kumar, K.S., Dahms, H.-U.-U., Lee, J.-S.-S., Kim, H.C., Lee, W.C., Shin, K.-H.-H., 2014. Algal photosynthetic responses to toxic metals and herbicides assessed by chlorophyll a fluorescence. Ecotoxicol. Environ. Saf. 104, 51–71. https://doi.org/10.1016/j.ecoenv.2014.01.042.

Kycko, M., Romanowska, E., Romanowska, Zagajewski B., 2019. Lead-induced changes in fluorescence and spectral characteristics of pea leaves. Remote Sens. 11 (16), 1885. https://doi.org/10.3390/rs11161885.

Lambert, A.-S.-S., Morin, S., Artigas, J., Volat, B., Coquery, M., Neyra, M., Pesce, S., 2012. Structural and functional recovery of microbial biofilms after a decrease in copper exposure: influence of the presence of pristine communities. Aquat. Toxicol. 109, 118–126.

Lavoie, M., Raven, J.A., Jones, O.A.H., Qiane, H., 2016. Energy cost of intracellular metal and metalloid detoxification in wild-type eukaryotic phytoplankton. Metallomics 8, 1097–1109. https://doi.org/10.1039/C6MT00049E.

Lawrence, J.R., Chenier, M.R., Roy, R., Beaumier, D., Fortin, N., Swerhone, G.D.W., Neu, T.R., Greer, C.W., 2004. Microscale and molecular assessment of impacts of nickel, nutrients, and oxygen level on structure and function of river biofilm communities. Appl. Environ. Microbiol. 70 (7), 4326–4339.

Lawson, J., 2005. River Basin Management. Progress Towards Implementation of the European Water Framework Directive. CRC Press, ISBN 9780415392006, 396 pp.

Margoum, C., Morin, S., Mazzella, N., 2015. Potential toxicity of pesticides in freshwater environments: passive sampling, exposure and impacts on biofilms: the PoToMAC project. Environ. Sci. Pollut. Res. 22, 3985–3987. https://doi.org/10.1007/s11356-014-3291-z.

Martínez-Ruiz, E.B., Martínez-Jerónimo, F., 2015. Nickel has biochemical, physiological, and structural effects on the green microalga *Ankistrodesmus falcatus*: an integrative study. Aquat. Toxicol. 169, 27–36.

Mykhaylenko, N.F., Zolotareva, E.K., 2017. The effect of copper and selenium nanocarboxylates on biomass accumulation and photosynthetic energy transduction efficiency of the green algae Chlorella vulgaris. Nanoscale Res. Lett. 12 (1), 147.

Nichols, H., Bold, H., 1965. Growth media-fresh water. In: Stein, J.R. (Ed.), Hand Book of Physiological. Methods. Cambridge University Press, Cambridge, pp. 7–24.
Nõges, P., Argillier, C., Borja, Á, Garmendia, J.M., Hanganu, J., Kodeš, V., Pletterbauer, F., Sagouis, A., Birk, S., 2016. Quantified biotic and abiotic responses to multiple stress in freshwater, marine and ground waters. Sci. Total Environ. 540 (1), 43–52. https://doi.org/10.1016/j.scitotenv.2015.06.045.
Pesce, S., Lissalde, S., Lavieille, D., Margoum, C., Mazzella, N., Roubeix, V., Montuelle, B., 2010. Evaluation of single and joint toxic effects of diuron and its main metabolites on natural phototrophic biofilms using a pollution-induced community tolerance (PICT) approach. Aquat. Toxicol. 99 (4), 492–499.
Pinto, J., Sigaud-Kutner, T.C.S., Leitão, M.A.S., Okamoto, O.K., Morse, D., Colepicolo, P., 2003. Heavy metal-induced oxidative stress in algae. J. Phycol. 39, 1008–1018.
Rodriguez Castro, M.C., Urrea, G., Guasch, H., 2014. Influence of the interaction between phosphate and arsenate on periphyton's growth and its nutrient uptake capacity. Sci. Total Environ. 503-504, 122–132. https://doi.org/10.1016/j.scitotenv.2014.06.094.
Roig, N., Sierra, J., Ortiz, J., Merseburger, G., Schuhmacher, M., Domingo, J.L., Nadal, M., 2013. Integrated study of metal behavior in Mediterranean stream ecosystems: a case study. J. Hazard. Mater. 263, 122–130. https://doi.org/10.1016/j.jhazmat.2013.07.051.
Roig, N., Sierra, J., Nadal, M., Moreno-Garrido, I., Nieto, E., Hampel, M., Pérez-Gallego, E., Schuhmacher, M., Blasco, J., 2015. Assessment of sediment ecotoxicological status as a complementary tool for the evaluation of surface water quality. The Ebro river basin case study. Sci. Total Environ. 503-504, 269–278. https://doi.org/10.1016/j.scitotenv.2014.06.125.
Sabater, S., Guasch, H., Ricart, M., Romaní, A.M., Vidal, G., Klünder, C., Schmitt-Jansen, M., 2007. Monitoring the effect of chemicals on biological communities. The biofilm as an interface. Anal. Bioanal. Chem. 387, 1425–1434.
Schmitt-Jansen, M., Altenburger, R., 2008. Community-level microalgal toxicity assessment by multiwavelength-excitation PAM fluorometry. Aquat. Toxicol. 86, 49–58.
Schreiber, U., 2004. Pulse-amplitude-modulation (PAM) fluorometry and saturation pulse method: an overview. In: Papageorgiou, G.C., Govindjee (Eds.), Chlorophyll a Fluorescence. Advances in Photosynthesis and Respiration, 19. Springer, Dordrecht Netherlands, pp. 279–319.
Serra, A., Guasch, H., 2009. Effects of chronic copper exposure on fluvial systems: linking structural and physiological changes on fluvial biofilms with the instream copper retention. Sci. Total Environ. 407, 5274–5282.
Serra, A., Corcoll, N., Guasch, H., 2009. Copper bioaccumulation and toxicity in fluvial periphyton: the influence of exposure history. Chemosphere 74, 633–664.
Serra, A., Guasch, H., Admiraal, W., Van der Geest, H.G., Van Beusekom, S.A.M., 2010. Influence of phosphorus on copper sensitivity of fluvial periphyton: the role of chemical, physiological and community-related factors. Ecotoxicology 19, 770–780.
Tiam, S.K., Morin, S., Bonet, B., Guasch, H., Feurtet-Mazel, A., Eon, M., Gonzalez, P., Mazzella, N., 2015. Is the toxicity of pesticide mixtures on river biofilm accounted for solely by the major compounds identified? Environ. Sci. Pollut. Res. 22 (6), 4009–4024.
Tuulaikhuu, B.-A.-A., Romaní, A.M., Guasch, H., 2015. Arsenic toxicity effects on microbial communities and nutrient cycling in indoor experimental channels mimicking a fluvial system. Aquat. Toxicol. 166, 72–82.
Uher, E., Besse, J.-P.-P., Delaigue, O., Husson, F., Lebrun, J.D., 2018. Comparison of the metal contamination in water measured by diffusive gradient in thin film (DGT), biomonitoring and total metal dissolved concentration at a national scale. Appl. Geochem. 88 (Part B), 247–257.
Xu, Y., Wang, C., Hou, J., Dai, S., Wang, P., Miao, L., Lv, B., Yang, Y., You, G., 2016. Effects of ZnO nanoparticles and Zn2+ on fluvial biofilms and the related toxicity mechanisms. Sci. Total Environ. 544, 230–237.
Yoshimasu, T., Ohashi, T., Oura, S., Kokawa, Y., Kawago, M., Hirai, Y., Miyasaka, M., Nishiguchi, H., Kawashiman, S., Yata, Y., Honda, M., Fujimoto, T., Okamura, Y., 2015. A theoretical model for the hormetic dose-response curve for anticancer agents. Anticancer Res. 35 (11), 5851–5855.